

# EPSP Amplification and the Precision of Spike Timing in Hippocampal Neurons

Desdemona Fricker\*<sup>†</sup> and Richard Miles

Laboratoire de Neurobiologie Cellulaire  
INSERM U261  
Institut Pasteur  
25 rue de Dr Roux  
75724 Paris  
France

## Summary

The temporal precision with which EPSPs initiate action potentials in postsynaptic cells determines how activity spreads in neuronal networks. We found that small EPSPs evoked from just subthreshold potentials initiated firing with short latencies in most CA1 hippocampal inhibitory cells, while action potential timing in pyramidal cells was more variable due to plateau potentials that amplified and prolonged EPSPs. Action potential timing apparently depends on the balance of subthreshold intrinsic currents. In interneurons, outward currents dominate responses to somatically injected EPSP waveforms, while inward currents are larger than outward currents close to threshold in pyramidal cells. Suppressing outward potassium currents increases the variability in latency of synaptically induced firing in interneurons. These differences in precision of EPSP–spike coupling in inhibitory and pyramidal cells will enhance inhibitory control of the spread of excitation in the hippocampus.

## Introduction

Excitatory postsynaptic potentials (EPSPs) are the basis for transmission of activity between synaptically connected neurons. The processes by which an EPSP causes a postsynaptic neuron to fire are therefore central to the operation of neural networks. The efficacy of EPSP–spike coupling depends on a number of factors, including the resting and threshold potential of a postsynaptic cell and the size and shape of the EPSP. Spike initiation may also depend on the activation of intrinsic conductances in dendritic and somatic membranes as well as at the site of action potential generation.

Subthreshold EPSPs may activate multiple intrinsic ionic conductances. Activation of inward currents tends to amplify EPSPs by increasing their amplitude and prolonging their decay. EPSP amplification in pyramidal cells of the hippocampus and neocortex (Stuart and Sakmann, 1995; Andreassen and Lambert, 1999) depends largely on axosomatically located sodium channels. EPSPs may also activate dendritic sodium (Lipowsky et al., 1996) and calcium channels (Gilllessen and Alzheimer, 1997). In contrast, the activation of outward

currents may counter the effects of inward currents on EPSP shape (Hoffman et al., 1997). Postsynaptic potassium currents can also accelerate EPSP decay in sympathetic ganglion cells (Cassell and McLachlan, 1986) and in granule cells of the olfactory bulb (Schoppa and Westbrook, 1999).

EPSP shaping by postsynaptic conductances is important in the integration of subthreshold synaptic signals. In pyramidal cells, for instance, EPSP amplification augments the efficacy of dendritic synapses, so compensating for an attenuation of distal events (Andreassen and Lambert, 1998). However, signaling at excitatory synapses also comprises a graded dimension of information coding that lies in the variability in timing of synaptically induced firing. At some junctions, including the Calyx of Held synapse (Brew and Forsythe, 1995) and synapses terminating on other auditory neurons (Koyano et al., 1996) and on spinal motoneurons (Fetz and Gustafsson, 1983), the timing of synaptically induced firing is precisely linked to that of the underlying EPSP. In contrast, EPSP–spike coupling seems to be much less precise in other neurons, including cortical pyramidal cells (Holt et al., 1996; Azouz and Gray, 1999), thalamic relay cells (Jahnsen and Llinas, 1984), and striatal spiny cells (Wickens and Wilson, 1998).

EPSP–spike coupling in the hippocampus shows high temporal fidelity at excitatory synapses onto some inhibitory cells (Miles, 1990; Csicsvari et al., 1998), although the underlying mechanisms are not clear. Less is known on the variability of coupling at synapses that excite pyramidal cells. We therefore began this study to compare the temporal precision with which small near-threshold EPSPs initiate spikes in hippocampal interneurons and pyramidal cells. The precision of EPSP–spike coupling was found to be correlated with EPSP amplification. Pyramidal cell EPSPs were prolonged at subthreshold potentials by the activation of a Na<sup>+</sup> current, and action potentials were initiated either by the EPSP rising phase or, at longer latencies, from a plateau potential. In contrast, inhibitory cell EPSPs showed little voltage-dependent amplification, and action potentials invariably arose from their rising phase. Voltage-clamp experiments using EPSP waveforms as command pulses showed that this difference results from outward currents that curtail EPSP amplification near threshold in inhibitory but not in pyramidal cells.

## Results

Somatic whole-cell recordings were made from 41 CA1 pyramidal cells and 43 interneurons located in the stratum radiatum of the CA1 area. Interneurons were identified by their morphological and electrical characteristics. Interneuron somata were round or fusiform and principal dendrites were oriented in stellate fashion rather than predominantly perpendicular to the stratum radiatum. The width of interneuron action potentials was  $0.9 \pm 0.2$  ms, consistently less than that of spikes generated by pyramidal cells which was  $1.5 \pm 0.5$  ms.

\*To whom correspondence should be addressed (e-mail: dfricker@bcm.tmc.edu).

<sup>†</sup>Present address: Department of Neuroscience, Baylor College of Medicine, Houston, Texas 77030.

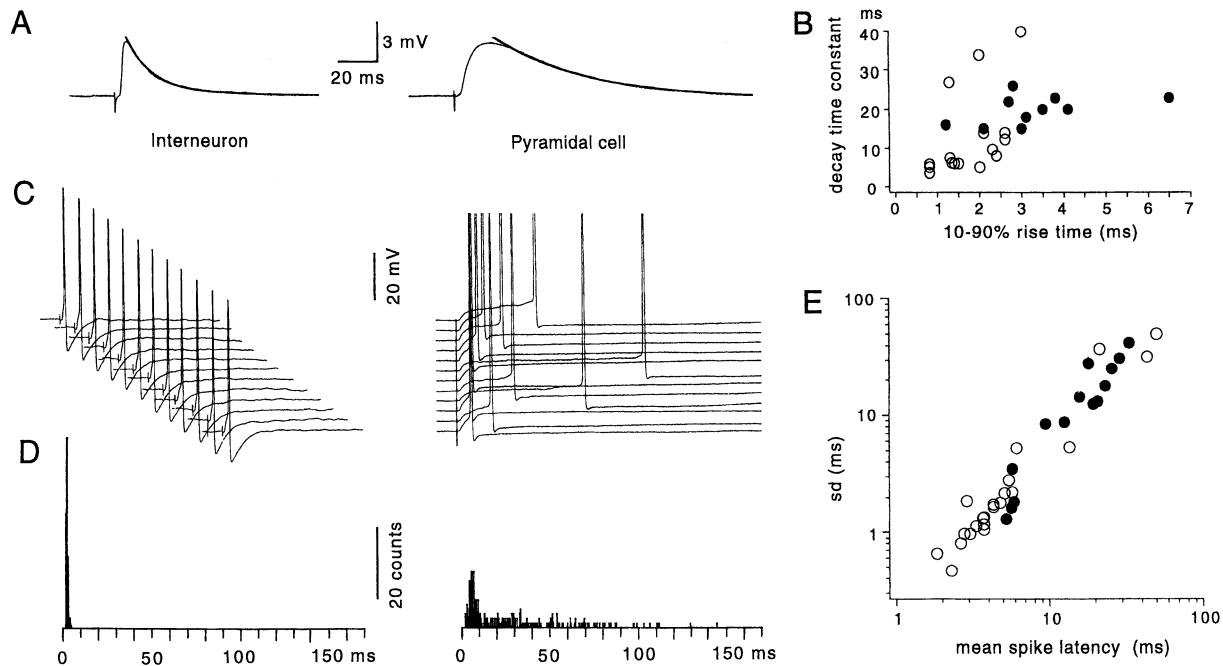


Figure 1. EPSP-Spike Coupling in Inhibitory and Pyramidal Cells

- (A) Evoked EPSPs in interneurons and pyramidal cells recorded at  $-80$  mV in the presence of bicuculline to block GABA-A receptor-mediated events, traces are averages of 20 trials. For the interneuron (left), the 10%–90% rise time was 0.8 ms, and its decay was fitted with a double exponential with time constants 5.8 and 30 ms; the values for the slower pyramidal EPSP (right) are 3.8 ms rise time and a single decay time constant of 23 ms.
- (B) Decay time constants plotted against 10%–90% rise time for EPSPs elicited in interneurons (open circles) and pyramidal cells (closed circles).
- (C) EPSP were always initiated from the rising phase of EPSPs in a typical interneuron (left), while in the pyramidal cell (right) spikes were often evoked after the peak of the EPSP. The threshold holding potential was  $-45$  mV (interneuron) and  $-50$  mV (pyramid).
- (D) Spike latency histograms constructed from the records of C ( $n = 112$  and  $n = 248$  trials, respectively).
- (E) Standard deviation of latency plotted against mean spike latencies for 14 pyramidal cells (closed circles) and 22 interneurons (open circles).

Small EPSPs of amplitude 3–5 mV were initiated by extracellular stimulation at distances of about  $50 \mu\text{m}$  from the soma of the recorded cell. EPSP kinetics, measured at  $-80$  mV to avoid activation of intrinsic conductances, were slower in pyramidal cells than in presumed interneurons (Debanne et al., 1995; Geiger et al., 1997). EPSP rise time (10%–90%) in interneurons was  $1.7 \pm 0.7$  ms and  $3.2 \pm 1.3$  ms in pyramidal cells. The decay of pyramidal cell EPSPs was best fitted by a monoexponential function with time constant of  $20 \pm 3.7$  ms. In most interneurons, a double exponential function was needed to obtain a satisfactory fit: the first, rapid time constant was  $8.0 \pm 3.6$  ms and the slower time constant was  $42 \pm 17$  ms. EPSPs in 3 putative interneurons possessed slower kinetics. Plotting EPSP decay time constant against their rise times revealed a good separation between interneuron and pyramidal cell populations (Figures 1A and 1B).

Our purpose in this study was to compare the coupling between EPSPs and action potentials in interneurons and CA1 pyramidal cells. This was accomplished by setting membrane potential to a level where EPSPs of amplitude 3–5 mV, evoked repetitively at 0.5–2 Hz, would initiate a single action potential with a probability of 0.3–0.7. Distributions of the latency of evoked action potentials were constructed from measurements of the delay between EPSP onset and action potential peak for

30–300 trials. In most interneurons spikes were initiated with little variability at short latencies corresponding to the rising phase of the EPSP. In contrast, the latency of action potential discharge in pyramidal cells was rather variable (Figures 1C and 1D). While most spikes were initiated during its rising phase, many action potentials arose at latencies of some 10s of ms from a plateau potential initiated by the EPSP. The mean EPSP–spike delay was  $8.95 \pm 13$  ms for interneurons (mean  $\pm$  SD;  $n = 22$ ) and was  $16.3 \pm 9$  ms for pyramidal cells ( $n = 14$ ). Eighteen of 22 interneurons had average spike delays below 6.1 ms ( $3.76 \pm 1.2$  ms,  $n = 18$ ), and we will refer to this subpopulation as “typical” interneurons. Overall, the variability in spike latency increased with the mean as shown in Figure 1E, which plots values for both pyramidal cells and interneurons.

The membrane holding potential from which EPSPs triggered cell firing in about 50% of the trials was  $-50 \pm 4$  mV for pyramidal cells and  $-45 \pm 6$  mV for interneurons. The threshold at which action potentials are initiated by EPSPs may be difficult to define. When firing occurs, an EPSP waveform leads to an action potential via a fast prepotential (Hu et al., 1992) and this transition often occurs without abrupt changes in slope of the membrane potential. Using a previous definition (Fricker et al., 1999) that the threshold is reached when membrane potential  $dV/dt$  exceeds 10 V/s, we derived thresh-

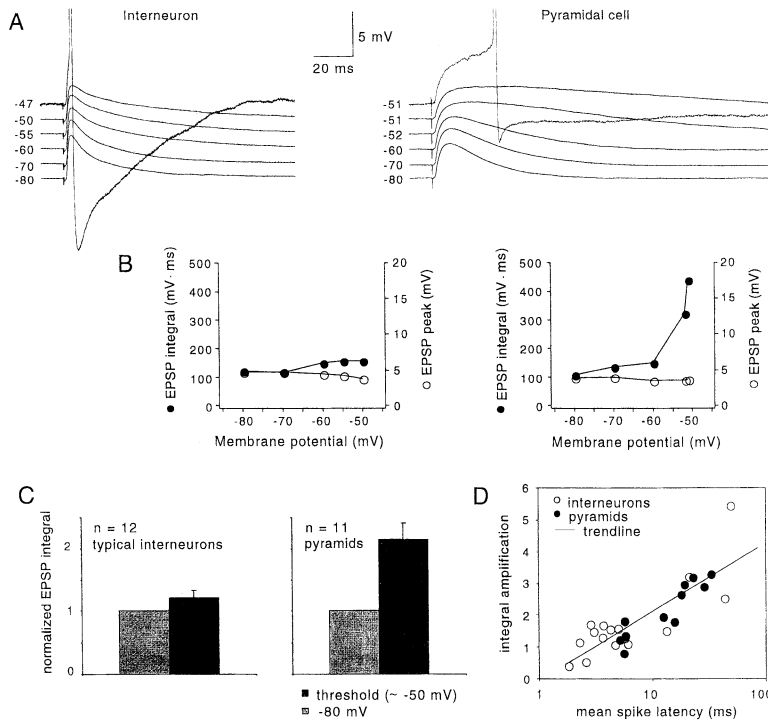


**Figure 2. Voltage Dependence of Interneuron and Pyramidal Cell EPSPs**

(A) Depolarization from  $-80$  mV to threshold prolonged EPSPs to a much greater extent in pyramidal cells than in interneurons. Near threshold plateau potentials give rise to long latency spikes in the pyramidal cell (right) but not in the interneuron (left).

(B) EPSP amplification quantified by plotting the EPSP integral (measured between onset and 160 ms, closed circles) and peak (open circles) against the holding potential. While the interneuron EPSP integral remains rather constant (left), the EPSP prolongation in the pyramidal cell translates into a 4-fold area increase close to threshold (right; data from same cells as in [A]). EPSP peak amplitude in both cell types decreased slightly with depolarization.

(C) Mean area increase in typical interneurons (left) and pyramids (right) at just threshold potentials normalized with respect to the EPSP integral measured at  $-80$  mV (error bars in this and the following figures indicate SEM).

(D) The degree of EPSP integral amplification is correlated with its mean latency of evoked spikes ( $n = 16$  interneurons, open circles;  $n = 11$  pyramidal cells, closed circles).

old potentials of  $-42 \pm 6$  mV for pyramidal cells and  $-38 \pm 6$  mV for interneurons.

### EPSP Kinetics and Voltage-Dependent Shaping of the EPSP

These data suggest that the variability in timing of spike initiation is correlated with a prolongation of EPSPs near threshold (Figures 1C and 1D), which is more marked in pyramidal cells than in inhibitory cells. EPSP form may be modified by the activation of voltage-dependent conductances in a postsynaptic cell. We therefore compared EPSP voltage dependence over the potential range between  $-80$  mV and firing threshold in both pyramidal and inhibitory cells (Figure 2). In all cells, EPSP amplitude tended to decrease with depolarization presumably due to a reduced driving force (Figure 2B). The decay of pyramidal cell, but not inhibitory cell, EPSPs was usually slowed with depolarization. EPSP time integrals have been used as an index of voltage-dependent amplification (Deisz et al., 1991; Stuart and Sakmann, 1995). We found that the area under inhibitory cell EPSPs increased by 18% when membrane potential was depolarized from  $-80$  to  $-50$  mV. In contrast, the integral of pyramidal cell EPSPs increased by 115% over the same potential range, largely due to a prolongation of their decay at subthreshold potentials. Voltage-dependent EPSP amplification measured with this index was strongly correlated with both the latency and the variability of evoked action potentials (Figure 2D).

### Spike Latency Is Correlated with EPSP Shape Modification by Intrinsic Currents

These data suggest that the activation of postsynaptic conductances modifies EPSP shape and so influences the temporal precision of action potential initiation.

EPSP amplification in pyramidal cells of hippocampus and neocortex has been attributed to the activation of perisomatic  $\text{Na}^+$  currents (Stuart and Sakmann, 1995; Andreasen and Lambert, 1999). However, it is difficult to test  $\text{Na}^+$  current involvement directly since suppressing  $\text{Na}^+$  currents with tetrodotoxin abolishes synaptic transmission. It seemed possible however, that the antiepileptic drug phenytoin, which blocks repeated  $\text{Na}^+$  channel openings (Kuo and Bean, 1994; Segal and Douglas, 1997), might suppress the currents that act to prolong EPSPs. We first verified that, at  $100\text{--}200 \mu\text{M}$ , phenytoin did not affect the amplitude or kinetics of the first action potential in a train induced by injecting depolarizing currents into CA1 pyramidal cells, while the amplitude of later spikes was strongly reduced ( $n = 4$ ; Figure 3A, inset). The actions of phenytoin were then tested on 10 pyramidal cell EPSPs that exhibited voltage-dependent amplification. In these cells, the increase in EPSP integrals on depolarization from  $-80$  to  $-50$  mV was reduced by 70% (Figure 3), largely due to an acceleration of EPSP decay at depolarized potentials. This data suggests that phenytoin reduced voltage-dependent EPSP amplification by suppressing a persistent  $\text{Na}^+$  current. The stability in peak EPSP amplitude measured at  $-80$  mV on exposure to phenytoin suggests that transmitter release from presynaptic terminals was not reduced. A residual voltage-dependent amplification observed in the presence of phenytoin (Figure 3) probably resulted from the activation of postsynaptic NMDA receptors since it was further reduced ( $n = 5$  cells) by application of the specific antagonist APV ( $100 \mu\text{M}$ ).

### Voltage-Dependent Amplification of Simulated EPSPs of Variable Shape

These data show that the voltage-dependent amplification of EPSPs in pyramidal cells depends in part on the

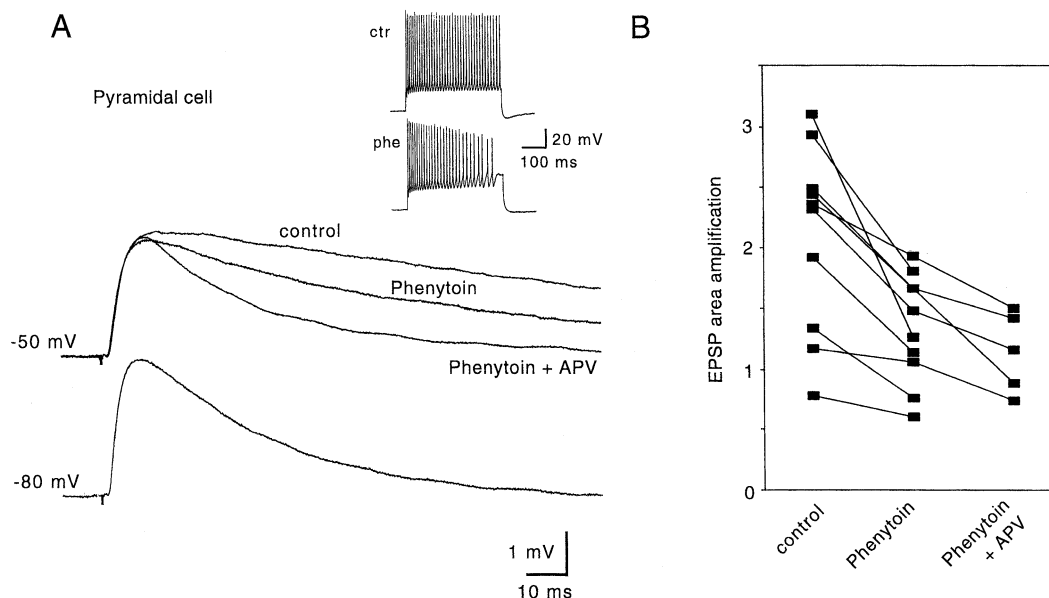


Figure 3. Phenytoin Acts to Reduce Pyramidal Cell EPSP Amplification

(A) Evoked EPSPs in control conditions at  $-80$  mV and close to threshold, then after bath application of  $200$   $\mu$ M Phenytoin and addition of  $100$   $\mu$ M APV (traces are average of 30 EPSPs).

(B) In all 10 pyramidal cells tested, phenytoin ( $100$ – $200$   $\mu$ M) reduced the EPSP amplification, suggesting that it partly results from the activation of a persistent sodium current. The remaining amplification is further reduced by APV ( $n = 5$ ), indicating a contribution of NMDA receptors.

activation of a  $\text{Na}^+$  conductance. Possibly rapid synaptic depolarizations, such as those in interneurons, activate inward currents less efficiently than the slower synaptic events that excite pyramidal cells. We addressed this question by injecting simulated EPSCs of different kinetics through a somatic recording electrode. This permitted the voltage-dependent amplification of fast and slow EPSP waveforms to be compared in the same cell and at the same time eliminated uncertainties in dendrosomatic transmission of synaptic events. Injected waveforms were chosen to mimic (1) a fast interneuron EPSP with rise time of  $1.7$  ms and a decay time constant of  $8.4$  ms and (2) a slower pyramidal cell EPSP with rise time  $3.2$  ms and decay time constant of  $20$  ms (see Experimental Procedures). Current waveforms were scaled during the recording to produce simulated EPSPs of amplitude close to  $5$  mV at  $-80$  mV.

EPSP waveforms simulated by somatic current injection were amplified in a similar way to synaptic events. Amplification in pyramidal cells, measured from the integrals of EPSP waveforms recorded at  $-50$  mV and at  $-80$  mV, ranged from  $80\%$  to  $380\%$  ( $n = 3$ ). Values of amplification between  $40\%$  and  $230\%$  were measured in 7 inhibitory cells. These values are larger than those obtained for evoked EPSPs at least in part since there is no reduction in driving force when current waveforms are compared at  $-80$  to  $-50$  mV, as there is when synaptic events are examined. Figure 4 shows also that in a given cell potential responses to injected synaptic waveforms with faster and slow kinetics were amplified to a similar extent. The mean amplification ratio for fast events divided by that for slow events was close to 1 in each cell tested and the mean value was  $1.07 \pm 0.28$  ( $n = 10$ ). Thus, postsynaptic currents underlying EPSP

amplification seem to be located close to the soma as in other neurons (Stuart and Sakmann, 1995) and are efficiently activated by EPSP-like depolarizations with either fast or slow kinetics.

#### The Balance of Inward and Outward Currents Activated by the EPSP

If the distinct kinetics of EPSPs impinging on interneurons and pyramidal cells do not explain the differential activation of  $\text{Na}^+$  currents, an alternative hypothesis is that EPSPs in interneurons might activate outward currents that act to oppose amplification. To test this possibility, we examined the inward and outward currents that were activated by command pulses with EPSP waveforms delivered in voltage-clamp records from pyramidal cells and interneurons (Figure 5). The test pulses used were of amplitude  $5$ – $20$  mV and possessed kinetics similar to typical pyramidal or inhibitory cell EPSPs (see Experimental Procedures). While no active currents were elicited at holding potentials of  $-80$  mV, both inward and outward currents were evoked at more depolarized potentials. We were especially interested to determine the balance of these currents near firing threshold. The holding potential was therefore adjusted to levels at which the EPSP waveform initiated an escape action current in about half the trials. This threshold holding potential was close to  $-51$  mV for pyramidal cells ( $n = 17$ ) and to  $-52$  mV for interneurons ( $n = 8$ ), although evidently the potential varied according to the amplitude of the injected EPSP waveform.

Voltage commands corresponding to a fast EPSP initiated a sequence of inward and outward currents in both interneurons and pyramidal cells (Figure 5). There was little difference in the peak amplitude of inward currents.

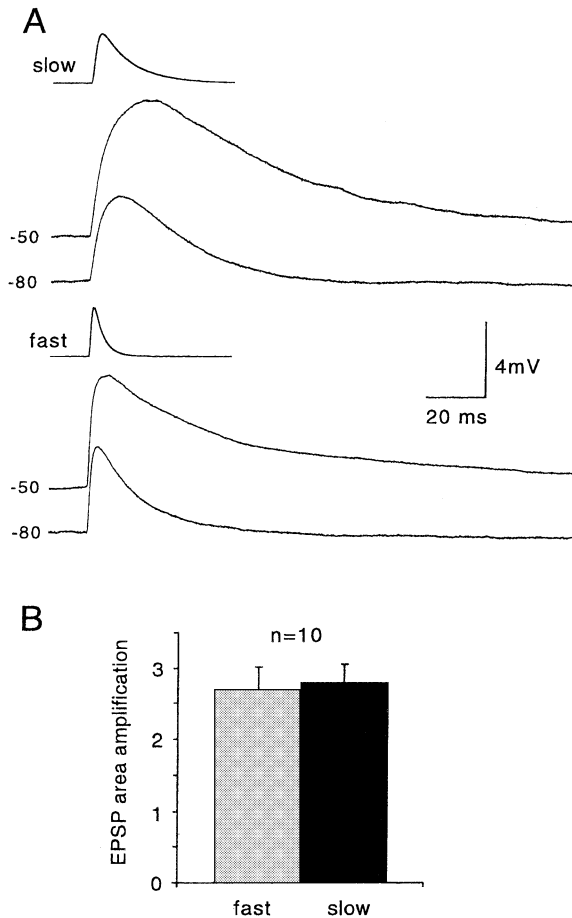


**Figure 4. Amplification Is Independent of EPSP Kinetics**  
(A) Voltage-dependent amplification of responses to somatic injection of EPSC waveforms of different kinetics in pyramidal cells ( $\tau_{on} = 0.6$  ms and  $\tau_{off} = 3$  ms for fast and  $\tau_{on} = 1.5$  ms and  $\tau_{off} = 10$  ms for slow EPSCs).  
(B) Membrane potential responses were amplified at depolarized potentials, suggesting that somatic voltage-dependent currents contribute to EPSP amplification and that their activation is not negligible for EPSPs with fast kinetics.

In pyramidal cells, it was  $-41 \pm 5$  pA, and in interneurons an inward current of  $-31 \pm 5$  pA was detected. In contrast, outward currents were systematically larger in interneurons,  $18 \pm 7$  pA, than in pyramidal cells,  $6 \pm 1$  pA. Inward currents were entirely blocked by the application of  $1 \mu\text{M}$  tetrodotoxin ( $n = 11$  cells) showing that they were carried by  $\text{Na}^+$  ions. Subtraction of traces before and after TTX application permitted comparison of the kinetics of inward and outward currents (Figure 5Ab). In both inhibitory and pyramidal cells, the onset of  $\text{Na}^+$  current activation (measured at 10% of the peak current) occurred at about 1.5 ms, corresponding closely to the peak of the simulated EPSP. An additional delay of 2 ms elapsed before the onset of  $\text{K}^+$  currents. The ratio of peak inward to outward current was 1.7 for interneurons, while in pyramidal cells the inward peak was 6.7 times greater than the peak outward current.

Since synaptic currents in the two cell types have distinctly different kinetics, we also examined how changing the kinetics of EPSP-like commands modified

the activation of inward and outward currents (Figure 6). Two waveforms were used, the first corresponding to an interneuron-like EPSP of time to peak 1.3 ms and decay time constant 5.5 ms, while the second was a pyramidal cell-like EPSP of time to peak 6 ms and decay time constant 22 ms. In pyramidal cells ( $n = 3$ ), the slower command initiated currents with slower kinetics and with a small decrease, from 8.3 to 6.3, in the ratio of the peak inward to outward current. However, slowing the kinetics of the EPSP waveform imposed on inhibitory cells ( $n = 4$ ) produced a proportionally larger outward current. Thus, slower synaptic events would be unlikely to reduce the temporal precision of EPSP–spike coupling in interneurons.

### K Currents Control the Precision of EPSP–Spike Coupling in Interneurons

This data suggests that both rapid synaptic currents and the activation of K currents contribute to the kinetics of threshold EPSPs in inhibitory cells and consequently underlie a high precision in the timing of evoked action potentials. This hypothesis was tested in experiments using evoked EPSPs. We first examined the effects of the potassium channel blockers 4-AP ( $20\text{--}40 \mu\text{M}$ ) and TEA ( $1\text{--}2$  mM) on the voltage dependence of EPSPs in interneurons ( $n = 5$ ). In the presence of these antagonists, EPSPs were prolonged in voltage-dependent fashion (Figure 7A). EPSP amplification measured from the ratio of integrals at  $-50$  and  $-80$  mV was increased from 15% to 88%. These experiments should be interpreted cautiously since in some recordings the peak amplitude of EPSPs at  $-80$  mV was increased suggesting that the antagonists acted presynaptically to enhance transmitter release. In these cases, stimulus intensity was reduced to maintain EPSP peak amplitude at  $-80$  mV, and holding potential was adjusted to maintain a similar probability of discharge as in control records. However, in the presence of K channel antagonists, near threshold EPSPs often initiated in inhibitory cells plateau potentials similar to those observed in pyramidal cells. Long latency action potentials could arise from these plateau potentials, although repetitive firing rarely occurred (Figure 7). These data thus suggest that  $\text{K}^+$  currents control the precision of EPSP–spike coupling in inhibitory cells.

### Physiological Significance of Delayed Firing in Pyramidal Cells

Our experiments on EPSP–spike coupling were carried out in the presence of picrotoxin or bicuculline to suppress synaptic inhibition. We also examined how IPSPs control pyramidal cell firing. In the absence of GABA-A receptor antagonists, focal stimulation initiated EPSPs that were succeeded in some trials (20%–75%) by disynaptic IPSPs with an additional latency of 2–4 ms (Figure 8A). When an IPSP was initiated, it prevented the generation of a plateau potential and abolished all synaptically initiated firing (Karnup and Stelzer, 1999). When inhibition was not activated, late firing occurred. These findings suggest that inhibitory circuits are an important site to control late synaptically driven firing in pyramidal cells. This control will operate stochastically and depend on the efficacy with which EPSPs induce inhibitory cell

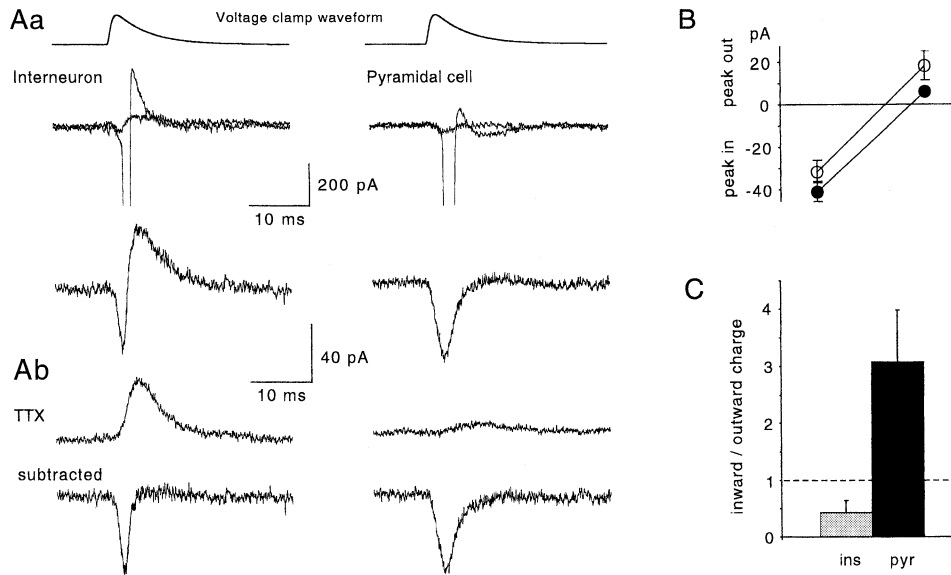


Figure 5. Intrinsic Inward and Outward Currents Activated by a Somatically Injected EPSP Waveform

(Aa) Voltage-clamp responses to somatic injection of a simulated EPSP waveform. Action currents escaped the voltage-clamp (upper traces) when the depolarization by the EPSP attained a membrane potential near  $-39$  mV in the interneuron and  $-43$  mV in the pyramidal cell. A sequence of an inward followed by an outward current is initiated in an interneuron (average from 30 trials, lower left), while outward currents are practically absent in the pyramidal cell (lower right).

(Ab) The outward current component could be isolated by bath application of TTX. The subtracted traces (lower) reveal the blocked inward current carried by sodium ions.

(B) The mixed inward and outward currents initiated at just subthreshold potentials show a lesser mean inward current component in interneurons (open circles,  $n = 8$ ) than pyramids (closed circles,  $n = 17$ ). Interneuron outward currents are larger than those in pyramidal cells.

(C) Charge transfer measured as current integrals from the TTX-separated inward and outward current components for 4 interneurons and 7 pyramidal cells. The mean ratio of the inward current integral over the outward current integral is significantly higher for pyramidal cells ( $p < 0.05$ ).

firing and consequently elicit disynaptic IPSPs in pyramidal cells.

We also examined the influence on EPSP–spike coupling in pyramidal cells of larger EPSPs such as may occur during synchronous afferent activities. Pyramidal cell holding potential was hyperpolarized, and EPSPs of three different amplitudes in the range 2–15 mV were used to trigger firing. As EPSP amplitude was increased, the probability of late discharges was reduced in a graded fashion (Figure 8B,  $n = 6$  cells).

## Discussion

We have shown that the temporal precision of action potential generation by EPSPs depends on the balance of inward and outward currents that they activate near to threshold. Thus, in hippocampal interneurons, small EPSPs evoked from just subthreshold potentials initiate action potentials with precise timing and short latencies, while in pyramidal cells, firing is initiated with longer and more variable delays. The narrow window for spike generation in interneurons seems to result from the activation of outward currents that prevent the generation of delayed spikes. In contrast, the balance between currents activated by pyramidal cell EPSPs favors inward sodium currents that underlie the plateau potentials that lead to long latency action potentials.

## Mechanisms Controlling EPSP Amplification

We found that the precision of EPSP–spike coupling (Figure 1) was closely correlated with a voltage-dependent prolongation of EPSP decay (Figure 2). This amplification occurred in pyramidal cells but was scarcely evident in interneurons. The effects of the  $\text{Na}^+$  channel antagonist phenytoin and responses to somatic injection of EPSC-like waveforms suggests that EPSP amplification in pyramidal cells depends largely on perisomatic  $\text{Na}^+$  currents (Stuart and Sakmann, 1995; Andreassen and Lambert, 1999).

The lack of amplification of interneuron EPSPs did not result from their rapid time course—somatically injected EPSP waveforms with fast and slow kinetics were amplified to a similar extent (Figure 4). Furthermore, voltage-clamp responses to EPSP-like command pulses indicate  $\text{Na}^+$  currents were activated to a similar degree at subthreshold potentials in interneurons and pyramidal cells (Figure 5). Interestingly, recent findings show a high  $\text{Na}^+$  current density in dendritic membrane of one group of hippocampal interneurons whose axons emerge from a principal dendrite at some distance from the soma (Martina et al., 2000). It seems, however, that differences in EPSP amplification result from differences in outward currents rather than in the density or distribution of inward currents (Figure 5). Suppressing outward currents revealed an amplification of inhibitory cell EPSPs and

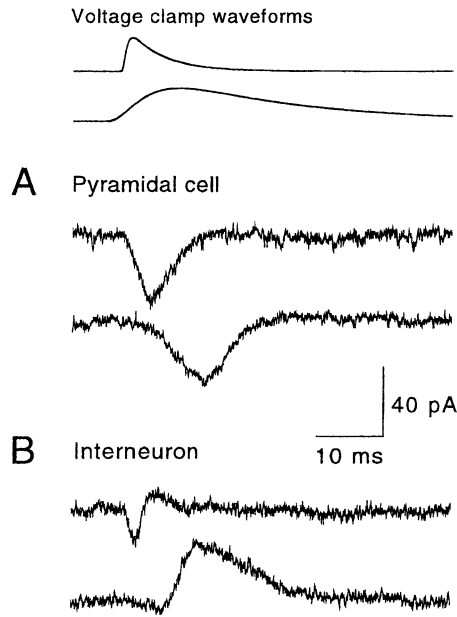


Figure 6. Fast and Slow Simulated EPSPs

Fast and slow simulated EPSP waveforms were used as voltage command in both interneurons and pyramidal cells. The fast EPSP was an interneuron-like event of rise time 1.3 ms and decay time constant 5.5 ms (upper); the slow EPSP was pyramidal cell-like event of rise time 6 ms and decay time constant 22 ms (lower).

(A) Switching from a fast to a slow EPSP in the pyramidal cell slowed the kinetics of the initiated inward current and slightly increased the delayed outward current component.

(B) Slowing the EPSP kinetics in an interneuron resulted in a proportionally stronger increase in the outward current component, suggesting that slower synaptic events would not alone reduce the precision of EPSP–spike coupling in interneurons.

greatly reduced the temporal precision with which action potentials were generated (Figure 7).

Our voltage-clamp experiments showed that K currents elicited by EPSP-like command pulses were larger at subthreshold potentials in interneurons than in pyramidal cells. Several factors could be involved—differences in threshold potential, or in the voltage dependence, the density or the identity of K currents. Our current and voltage-clamp experiments revealed only small differences in inhibitory and pyramidal cell threshold. The molecular identity of subthreshold K channels expressed in pyramidal cells and in subsets of interneurons is different (Serodio and Rudy, 1998), but the voltages at which A-type K currents are activated seem to be rather similar (Numann et al., 1987; Zhang and McBain, 1995; Hoffman et al., 1997; Martina et al., 1998). The data of Figure 8B suggests that K current inactivation may exert a graded control on the occurrence of late firing in pyramidal cells. If so, the rate of synaptic depolarization to threshold, which controls the rate of transition of K channels into their inactivated state (Fricker et al., 1999), may critically determine the precision of EPSP–spike timing in pyramidal cells. However, EPSP–spike timing in inhibitory cells is precise when K channels are functional (Figure 7). The key difference between inhibitory and pyramidal cells may be the density of somatic expression of K channels. Comparative stud-

ies using both nucleated patch (Martina et al., 1998) and cell attached records (Fricker et al., 1999) suggest that inhibitory cell K currents are larger than those of pyramidal cells. Our data suggest that while these voltage-gated K channels control the falling phase of EPSPs on interneurons, they are not activated quickly enough to influence the rising phase (Figure 5).

#### Mechanisms for Spike Initiation

We have demonstrated two distinct regimes for action potential initiation. In most interneurons, spikes were triggered with little variability and short latencies from the rising phase of the EPSP. This behavior resembles the initiation of action potentials in motoneurons (Coombs et al., 1955; Fetz and Gustafsson, 1983), where the form of latency histograms of synaptically evoked spikes is similar to the temporal derivative of the EPSP and threshold is typically crossed during the rising slope (Knox, 1974). A similar preference for spike initiation from depolarizing transients has been reported in neocortical pyramidal cells (Mainen and Sejnowski, 1995).

Action potential initiation in CA1 pyramidal cells differed from that in interneurons. While some spikes were triggered from the rising phase of an EPSP, a significant proportion of long latency spikes arose from plateau potentials that prolonged EPSPs. The initiation of long latency spikes was not associated with a rapid change in postsynaptic membrane potential. Rather, the moment for action potential discharge depends on the extent and time course of EPSP amplification, and therefore on the balance between intrinsic postsynaptic conductances. The variability in timing of spikes that arise from plateau potentials is reminiscent of that observed in responses to DC current pulses (Mainen and Sejnowski, 1995) and presumably reflects the stochastic nature of ion channel behavior near threshold. Stochastic effects will depend on the number of channels available near firing threshold (Schneidman et al., 1998). Due to voltage-dependent inactivation, the availability of both  $\text{Na}^+$  and  $\text{K}^+$  currents in hippocampal neurons near threshold is 20%–30% (Fricker et al., 1999), suggesting that current fluctuations may be significant (Sigworth, 1980; White et al., 1998).

#### Functional Implications of Precise and Imprecise Spike Timing

EPSPs initiate firing with high temporal precision at certain synapses, often close to the periphery. These connections include excitatory synapses made with spinal motoneurons (Fetz and Gustafsson, 1983) where spike timing is presumably important for the generation of precisely coordinated motor outputs. In sensory systems, too, the time-locking of firing to peripheral events may be preserved across at least one synapse. At the Calyx of Held synapse with neurons of the trapezoid body nucleus, auditory information is transformed into postsynaptic firing with the high precision needed for sound source localization (Brew and Forsythe, 1995).

We have shown that EPSP–spike coupling is precise in the majority of hippocampal inhibitory cells. Differences in interneuron behavior—in 4 out of 22 inhibitory cells coupling was notably less precise—may reflect the variability in this cell population (Parra et al., 1998) or

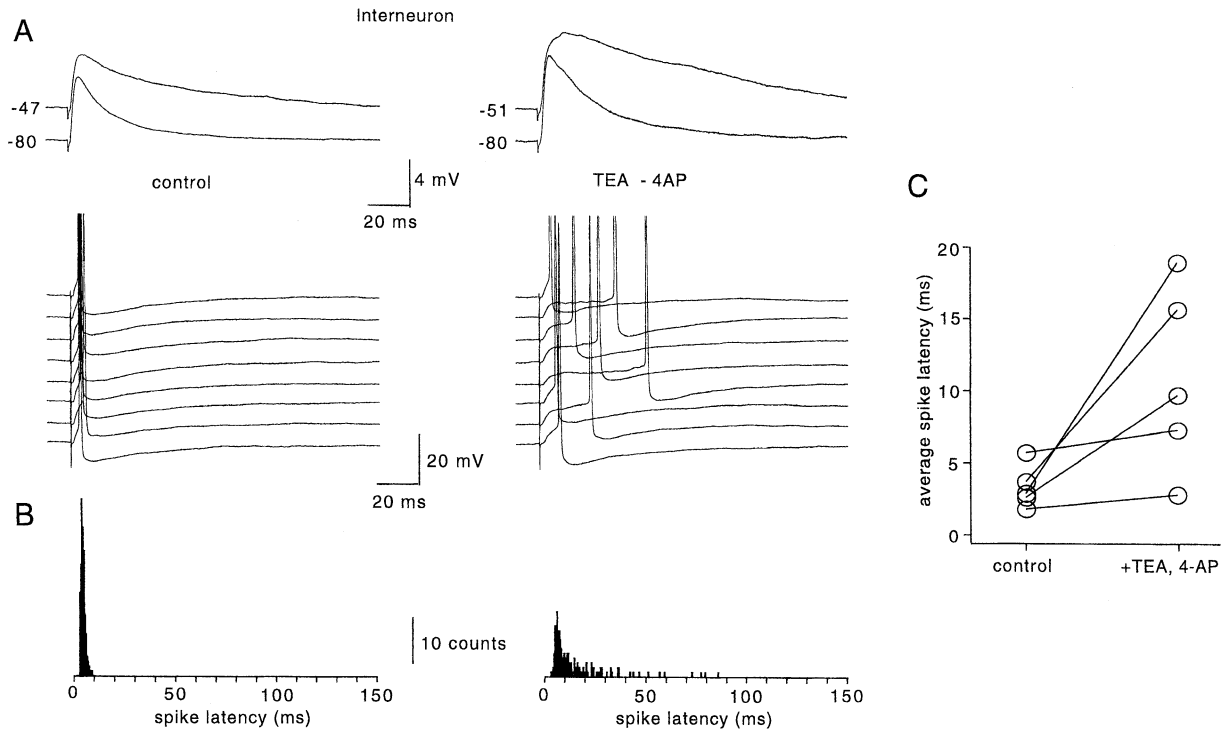


Figure 7. K Channel Blockers Prolong EPSP Decay and Lead to Delayed Spikes in Interneurons

(A) Evoked EPSPs in control conditions and after bath application of 40 mM 4-AP and 1 mM TEA at  $-80$  mV and close to threshold. K channel blockers uncovered a voltage-dependent amplification of subthreshold EPSPs and a loss of temporal precision in EPSP-spike coupling. (B) Spike latency histograms in control conditions and in the presence of K channel blockers each constructed from 175 spikes. (C) In all interneurons tested, EPSP amplification in the presence of TEA and 4-AP led to delayed spikes with increased mean latency.

possibly a misidentification of elements with somata located in stratum radiatum (Gulyas et al., 1998). The rapid and effective excitation of inhibitory cells may permit them to act as coincidence detectors (Softky, 1995). It also implies that synaptic inhibition will be quickly

and efficiently activated in response to any increase of activity in pyramidal cell populations.

The variability in timing of synaptically induced discharges in pyramidal cells seems at first more puzzling (Stuart and Sakmann, 1995). Neuronal codes that de-

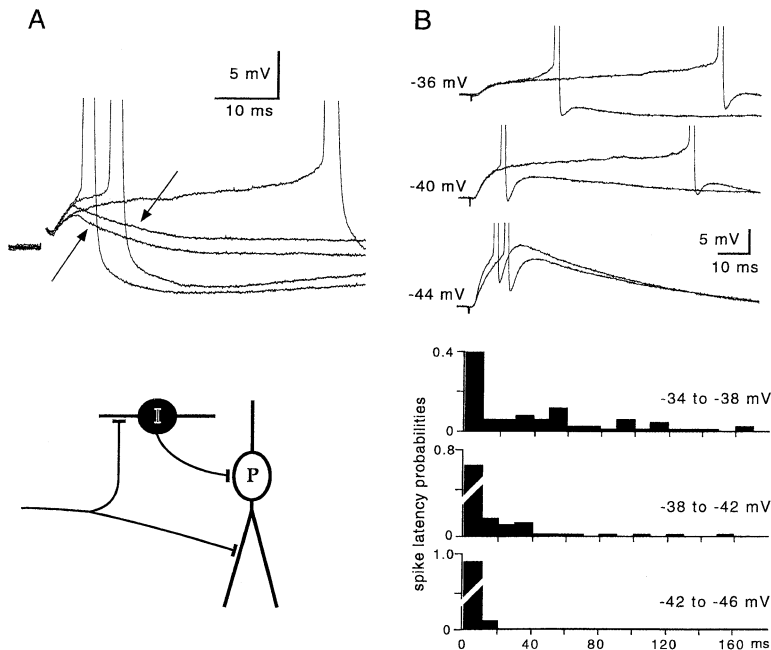


Figure 8. Influence of Synaptic Inhibition and EPSP Amplitude on Precision of EPSP-Spike Coupling in Pyramidal Cells

(A) Focal stimulation in the absence of blockers at receptors at inhibitory synapses initiated either an EPSP that could initiate firing or an EPSP-IPSP sequence. In this recording IPSPs (arrows) were initiated in 103 of 164 trials. When an IPSP was elicited, the pyramidal cell did not discharge. The inset shows the synaptic circuit underlying the occurrence of monosynaptic EPSPs and disynaptic IPSPs. (B) Variation of the temporal precision of firing with EPSP amplitude and holding potential. In this experiment, responses to EPSPs of amplitudes 2–3, 5–7, and 10–12 mV were examined. Postsynaptic holding potential was adjusted so that firing was induced with a probability of about 0.5. Late firing was defined as the proportion of synaptic events occurring at latencies longer than 10 ms. Histograms of the distribution of spike latencies for at each holding potential show that the proportion of delayed action potentials was reduced in graded fashion as EPSP amplitude increased.

pend on spike timing require temporal precision, so if the synchronous discharge of ensembles of pyramidal cells is involved in perceptual grouping (Singer, 1999), then their firing should be precisely linked to afferent synaptic events. Our findings suggest that for the small EPSPs that we tested, EPSP–spike coupling in pyramidal cells is not precise. Delayed spiking may be advantageous in some situations—for example, to maintain reverberating discharges in pyramidal cell ensembles with recurrent connectivity (Wang, 1999). The inhibitory control of late pyramidal cell firing shown in Figure 8A suggests that changes in the efficacy of inhibitory circuits will control the extent of reverberating activities in pyramidal cell populations. It is interesting that phenytoin, which suppressed EPSP amplification, is an anticonvulsant drug, suggesting that delayed spiking may also have pathological consequences.

Is EPSP–spike coupling in pyramidal cells temporally imprecise in all physiological conditions? In this study, we examined the effects of small EPSPs evoked from just subthreshold potentials, but Figure 8B shows that the variability in spike latency was reduced as larger EPSPs were elicited from more hyperpolarized potentials. Hyperpolarization probably removed K current inactivation, reducing EPSP prolongation by intrinsic currents and so suppressing delayed firing. Thus, the state of K current inactivation preceding a unitary EPSP that triggers pyramidal cell firing will be crucial determinant of the temporal precision of EPSP–spike coupling. This parameter will depend on the potential trajectory preceding the last unitary EPSP. At near-threshold potentials, pyramidal cell K channels inactivate with a time constant of 10–20 ms (Numann et al., 1987; Martina et al., 1998; Fricker et al., 1999). Large summed EPSPs with fast rise times, which may occur in some pathological and physiological states, may then initiate firing rather precisely. In other behavioral states, including the theta rhythm with a period of 100–200 ms, pyramidal cells fire in response to slower asynchronous EPSP sequences. The final, unitary EPSP that triggers firing is likely to arrive at a membrane potential at which K currents are relatively inactivated, as in our experimental conditions, and EPSP–spike coupling seems likely to be imprecise.

Our results have shown that EPSPs are coupled to action potential generation in both pyramidal and inhibitory cells via the activation of both intrinsic inward and outward voltage-gated conductances. Short-term (Chen and Wong, 1991; Astman et al., 1998; Hoffman and Johnston, 1998) or long-term changes (Desai et al., 1999) in these currents, could modify both the efficacy (Chavez-Noriega et al., 1990) and the temporal precision of information transfer at synapses. The consequences of such a regulation for network function remain to be explored.

#### Experimental Procedures

##### Slices

Experiments were performed (according to local regulations) on hippocampal slices obtained from 11- to 26-day-old Sprague-Dawley rats. The animals were anaesthetized by intraperitoneal injection of ketamine (200 mg/kg) and chloral hydrate (800 mg/kg) and then perfused intracardially with ice-cold solution containing (in mM) NaCl 130, KCl 2.0, CaCl<sub>2</sub> 2, MgCl<sub>2</sub> 2, NaH<sub>2</sub>PO<sub>4</sub> 1.3, NaHCO<sub>3</sub>

20, and glucose 27.7. After decapitation, the hippocampal formation was removed from the brain and cut into 300 μm thick transverse slices using a tissue slicer (Dosaka, Kyoto, Japan). Slices were kept at room temperature in the same saline bubbled with a mixture of 95% O<sub>2</sub> and 5% CO<sub>2</sub>, before being transferred into a heated recording chamber (34°C).

##### Solutions

The slices were continuously superfused with a solution containing (in mM): NaCl 130, KCl 2.0, CaCl<sub>2</sub> 2, MgCl<sub>2</sub> 2, NaH<sub>2</sub>PO<sub>4</sub> 1.3, NaHCO<sub>3</sub> 20, glucose 27.7, and saturated with 95% O<sub>2</sub> and 5% CO<sub>2</sub>. Bicuculline (30 μM) or picrotoxin (50 μM) was routinely added to the perfusing solution to block inhibitory synaptic activity. Drugs were applied by bath application. The time to exchange the solution in the recording chamber was 30 s, as measured from the change in junction potential of an open electrode on switching between extracellular saline and distilled water. Pipettes were filled with solutions containing (in mM) K-gluconate 130, KCl 10, EGTA 10, MgCl<sub>2</sub> 2, HEPES 5, and KOH to adjust to pH 7.3. In some experiments, K-gluconate was replaced by KCl or by K-methylsulphonate with no apparent effect on our results. Phenytoin (diphenyl hydantoin, 200 μM) was added to the solution to suppress Na<sup>+</sup> currents and 1 mM tetraethyl ammonium (TEA) and 20 μM 4 aminopyridine (4-AP) were used to suppress K currents. D,L-2-amino-5-phosphonvaleric acid (APV, 100 μM) was added in some experiments to suppress synaptic currents mediated via NMDA receptors. All chemicals were purchased from Sigma.

##### Recordings

Patch pipettes were pulled from borosilicate glass of external diameter 1.5 mm (Hilgenberg, Malsfeld, Germany) using a Brown-Flaming electrode puller (Sutter Instruments). Their resistance when filled with recording solution varied from 3 to 5 MΩ. Records were made from pyramidal cells and from interneurons with somata in stratum radiatum of the CA1 area. Cells were identified visually using a Nikon microscope equipped with a differential interference contrast (DIC) optics and a 40× objective. Slices were illuminated with light passed through a filter (high-pass, cut-off 700 nm) that was detected by a camera sensitive to infrared (Hamamatsu C3077).

Whole-cell records were made with an Axopatch 200A amplifier, using the “fast CC mode” for current clamp recordings. Stimulation and data acquisition was controlled by pCLAMP 6 software (Axon Instruments). Signals were filtered at 5 kHz and stored on a DAT Biologic tape recorder. They were digitized with a Labmaster interface (Axon Instruments) at a sampling interval of 20 μs. Leakage and capacitive currents were subtracted online using a p/–4 protocol (four negative correction pulses, amplitude 1/4 of the test pulse).

For whole-cell recordings, the amplifier was zeroed with the recording pipette in the bath solution to null the junction potential between the bath and the pipette solution. The pipette was then advanced through the slice under positive pressure, and when the approaching electrode was seen to distort the cell body, negative pressure was applied to form a seal of resistance greater than 1 GΩ between the electrode and the cell. Whole-cell current clamp recordings were established by applying a brief pulse of suction after seal formation to obtain access to the cell cytoplasm. Input resistance in the whole-cell configuration was 150–400 MΩ and was checked repeatedly during a recording by measuring the voltage response to a hyperpolarizing current pulse of 0.1 nA amplitude.

##### Stimulation

EPSPs were evoked by bipolar stimulation electrodes placed at a distance of 30–50 μm from the soma of the recorded neuron. Stimulation strength was adjusted to yield small EPSPs with apparently monoexponential decay and amplitude less than 5 mV at –80 mV. IPSPs were suppressed with bicuculline, but we did not distinguish between AMPA- and NMDA-mediated components of EPSPs. Stimulations were repeated at a frequency of 0.5–2 Hz, which did not induce persistent changes in EPSP amplitude. Latency distributions for action potentials induced by these small EPSPs were constructed from at least 30 responses to synaptic events elicited at holding potentials just below threshold so that spikes were initiated in 30%–60% of trials. Changing holding potential in a range of ±2

mV increased or decreased discharge probability but did not change the pattern of spike latency distributions. In some cells spikes could not be evoked by EPSPs without the occurrence of frequent spontaneous action potentials between the stimulations. Those cells were not used for analysis. Spontaneously active cells were slightly hyperpolarized to determine their threshold potential.

#### Use of Simulated Synaptic Waveforms

In current clamp, EPSCs were simulated by somatic injection of an exponentially rising and falling voltage waveform  $f(t) = a \cdot ((1 - \exp(-t / \tau_{\text{on}}))^{\beta}) \cdot \exp(-t / \tau_{\text{off}})$ . For fast simulated events,  $\tau_{\text{on}}$  was 0.6 ms and  $\tau_{\text{off}}$  was 3 ms; for slow events  $\tau_{\text{on}}$  was 1.5 ms and  $\tau_{\text{off}}$  was 10 ms. In voltage-clamp experiments, EPSP-like commands were simulated using the same equation. For fast EPSP-like waveforms,  $\tau_{\text{on}}$  was 1.5 ms and  $\tau_{\text{off}}$  was 10 ms, and for slow events  $\tau_{\text{on}}$  was 8 ms and  $\tau_{\text{off}}$  was 40 ms.

#### Acknowledgments

This work was supported by INSERM and the NIH (MH54671). We thank I. Cohen for help with the analysis.

Received March 8, 2000; revised September 15, 2000.

#### References

- Andreasen, M., and Lambert, J.D. (1998). Factors determining the efficacy of distal excitatory synapses in rat hippocampal CA1 pyramidal neurones. *J. Physiol. Lond.* **507**, 441–462.
- Andreasen, M., and Lambert, J.D. (1999). Somatic amplification of distally generated subthreshold EPSPs in rat hippocampal pyramidal neurones. *J. Physiol. Lond.* **519**, 85–100.
- Astman, N., Gutnick, M.J., and Fleidervish, I.A. (1998). Activation of protein kinase C increases neuronal excitability by regulating persistent Na<sup>+</sup> current in mouse neocortical slices. *J. Neurophysiol.* **80**, 1547–1551.
- Azouz, R., and Gray, C.M. (1999). Cellular mechanisms contributing to response variability of cortical neurons in vivo. *J. Neurosci.* **19**, 2209–2223.
- Brew, H.M., and Forsythe, I.D. (1995). Two voltage-dependent K<sup>+</sup> conductances with complementary functions in postsynaptic integration at a central auditory synapse. *J. Neurosci.* **15**, 8011–8022.
- Cassell, J.F., and McLachlan, E.M. (1986). The effect of a transient outward current (I<sub>A</sub>) on synaptic potentials in sympathetic ganglion cells of the guinea-pig. *J. Physiol. Lond.* **374**, 273–288.
- Chavez-Noriega, L.E., Halliwell, J.V., and Bliss, T.V. (1990). A decrease in firing threshold observed after induction of the EPSP-spike (E-S) component of long-term potentiation in rat hippocampal slices. *Exp. Brain Res.* **79**, 633–641.
- Chen, Q.X., and Wong, R.K. (1991). Intracellular Ca<sup>2+</sup> suppressed a transient potassium current in hippocampal neurons. *J. Neurosci.* **11**, 337–343.
- Coombs, J.S., Eccles, J.C., and Fatt, P. (1955). Excitatory synaptic action in motoneurons. *J. Physiol. Lond.* **130**, 374–395.
- Csicsvari, J., Hirase, H., Czurko, A., and Buzsaki, G. (1998). Reliability and state dependence of pyramidal cell-interneuron synapses in the hippocampus: an ensemble approach in the behaving rat. *Neuron* **21**, 179–189.
- Debanne, D., Guerineau, N.C., Gahwiler, B.H., and Thompson, S.M. (1995). Physiology and pharmacology of unitary synaptic connections between pairs of cells in areas CA3 and CA1 of rat hippocampal slice cultures. *J. Neurophysiol.* **73**, 1282–1294.
- Deisz, R.A., Fortin, G., and Zieglgansberger, W. (1991). Voltage dependence of excitatory postsynaptic potentials of rat neocortical neurons. *J. Neurophysiol.* **65**, 371–382.
- Desai, N.S., Rutherford, L.C., and Turrigiano, G.G. (1999). Plasticity in the intrinsic excitability of cortical pyramidal neurons. *Nat. Neurosci.* **2**, 515–520.
- Fetz, E.E., and Gustafsson, B. (1983). Relation between shapes of post-synaptic potentials and changes in firing probability of cat motoneurons. *J. Physiol. Lond.* **341**, 387–410.
- Fricker, D., Verheugen, J.A., and Miles, R. (1999). Cell-attached measurements of the firing threshold of rat hippocampal neurones. *J. Physiol. Lond.* **517**, 791–804.
- Geiger, J.R., Lubke, J., Roth, A., Frotscher, M., and Jonas, P. (1997). Submillisecond AMPA receptor-mediated signaling at a principal neuron-interneuron synapse. *Neuron* **18**, 1009–1023.
- Gillessen, T., and Alzheimer, C. (1997). Amplification of EPSPs by low Ni(2<sup>+</sup>)- and amiloride-sensitive Ca<sup>2+</sup> channels in apical dendrites of rat CA1 pyramidal neurons. *J. Neurophysiol.* **77**, 1639–1643.
- Gulyas, A.I., Toth, K., McBain, C.J., and Freund, T.F. (1998). Stratum radiatum giant cells: a type of principal cell in the rat hippocampus. *Eur. J. Neurosci.* **10**, 3813–3822.
- Hoffman, D.A., and Johnston, D. (1998). Downregulation of transient K<sup>+</sup> channels in dendrites of hippocampal CA1 pyramidal neurons by activation of PKA and PKC. *J. Neurosci.* **18**, 3521–3528.
- Hoffman, D.A., Magee, J.C., Colbert, C.M., and Johnston, D. (1997). K<sup>+</sup> channel regulation of signal propagation in dendrites of hippocampal pyramidal neurons. *Nature* **387**, 869–875.
- Holt, G.R., Softky, W.R., Koch, C., and Douglas, R.J. (1996). Comparison of discharge variability in vitro and in vivo in cat visual cortex neurons. *J. Neurophysiol.* **75**, 1806–1814.
- Hu, G.Y., Hvalby, O., Lacaille, J.C., Piercey, B., Ostberg, T., and Andersen, P. (1992). Synaptically triggered action potentials begin as a depolarizing ramp in rat hippocampal neurones in vitro. *J. Physiol.* **453**, 663–687.
- Jahnsen, H., and Llinas, R. (1984). Electrophysiological properties of guinea-pig thalamic neurones: an in vitro study. *J. Physiol. Lond.* **349**, 205–226.
- Karnup, S., and Stelzer, A. (1999). Temporal overlap of excitatory and inhibitory afferent input in guinea pig CA1 pyramidal cells. *J. Physiol.* **516**, 485–504.
- Knox, C.K. (1974). Cross-correlation functions for a neuronal model. *Biophys. J.* **14**, 567–582.
- Koyano, K., Funabiki, K., and Ohmori, H. (1996). Voltage-gated ionic currents and their roles in timing coding in auditory neurons of the nucleus mesencephalicus profundus of the chick. *Neurosci. Res.* **26**, 29–45.
- Kuo, C.C., and Bean, B.P. (1994). Na channels must deactivate to recover from inactivation. *Neuron* **12**, 819–829.
- Lipowsky, R., Gillessen, T., and Alzheimer, C. (1996). Dendritic Na<sup>+</sup> channels amplify EPSPs in hippocampal CA1 pyramidal cells. *J. Neurophysiol.* **76**, 2181–2191.
- Mainen, Z.F., and Sejnowski, T.J. (1995). Reliability of spike timing in neocortical neurons. *Science* **268**, 1503–1506.
- Martina, M., Schultz, J.H., Ehmke, H., Monyer, H., and Jonas, P. (1998). Functional and molecular differences between voltage-gated K<sup>+</sup> channels of fast-spiking interneurons and pyramidal neurons of rat hippocampus. *J. Neurosci.* **18**, 8111–8125.
- Martina, M., Vida, I., and Jonas, P. (2000). Distal initiation and active propagation of action potentials in interneuron dendrites. *Science* **287**, 295–300.
- Miles, R. (1990). Synaptic excitation of inhibitory cells by single CA3 hippocampal pyramidal cells of the guinea-pig in vitro. *J. Physiol. Lond.* **428**, 61–77.
- Numann, R.E., Wadman, W.J., and Wong, R.K. (1987). Outward currents of single hippocampal cells obtained from the adult guinea-pig. *J. Physiol. Lond.* **393**, 331–353.
- Parra, P., Gulyas, A.I., and Miles, R. (1998). How many subtypes of inhibitory cells in the hippocampus? *Neuron* **20**, 983–993.
- Schneidman, E., Freedman, B., and Segev, I. (1998). Ion channel stochasticity may be critical in determining the reliability and precision of spike timing. *Neural Comput.* **10**, 1679–1703.
- Schoppa, N.E., and Westbrook, G.L. (1999). Regulation of synaptic timing in the olfactory bulb by an A-type potassium current. *Nat. Neurosci.* **2**, 1106–1113.
- Segal, M.M., and Douglas, A.F. (1997). Late sodium channel open-

- ings underlying epileptiform activity are preferentially diminished by the anticonvulsant phenytoin. *J. Neurophysiol.* *77*, 3021–3034.
- Serodio, P., and Rudy, B. (1998). Differential expression of Kv4 K<sup>+</sup> channel subunits mediating subthreshold transient K<sup>+</sup> (A-type) currents in rat brain. *J. Neurophysiol.* *79*, 1081–1091.
- Sigworth, F.J. (1980). The variance of sodium current fluctuations at the node of Ranvier. *J. Physiol. Lond.* *307*, 97–129.
- Singer, W. (1999). Neuronal synchrony: a versatile code for the definition of relations? *Neuron* *24*, 49–65.
- Softky, W.R. (1995). Simple codes versus efficient codes. *Curr. Opin. Neurobiol.* *5*, 239–247.
- Stuart, G., and Sakmann, B. (1995). Amplification of EPSPs by axosomatic sodium channels in neocortical pyramidal neurons. *Neuron* *15*, 1065–1076.
- Wang, X.J. (1999). Synaptic basis of cortical persistent activity: the importance of NMDA receptors to working memory. *J. Neurosci.* *19*, 9587–9603.
- White, J.A., Klink, R., Alonso, A., and Kay, A.R. (1998). Noise from voltage-gated ion channels may influence neuronal dynamics in the entorhinal cortex. *J. Neurophysiol.* *80*, 262–269.
- Wickens, J.R., and Wilson, C.J. (1998). Regulation of action-potential firing in spiny neurons of the rat neostriatum in vivo. *J. Neurophysiol.* *79*, 2358–2364.
- Zhang, L., and McBain, C.J. (1995). Voltage-gated potassium currents in stratum oriens-alveus inhibitory neurones of the rat CA1 hippocampus. *J. Physiol. Lond.* *488*, 647–660.